Raj Kumar Pathak 2025, 13:4
ISSN (Online): 2348-4098
ISSN (Print): 2395-4752

International Journal of Science, Engineering and Technology

An Open Access Journal

Parametric Optimization and Their Effect on Mechanical Properties of Friction Stir Welded AA1100 Aluminum Alloy

Raj Kumar Pathak, Tanvir Singh

Abstract- This research work deals with studying the effect of welding parameters on the mechanical and metallurgical properties of friction stir-welded joints of AA1100 aluminum alloy. FSW process parameters with tool rotational speed range from 1400 to 1800 rpm and traverse speeds from 80 to 120 mm/min were employed. Results revealed that higher ultimate tensile stress (127 MPa–148 MPa) and percentage elongation (1.9- 11%) with joint efficiency (82-95%) for every set of rotational speed and traverse speed compared to the base material (155 MPa, 75MPa and 12% of ultimate tensile strength, yield strength and % elongation, respectively). The joint efficiency of most of the samples is around 70–80 % with the highest joint efficiency of 95.64% of FSW welds produced at 1800 rpm and 100 mm/min of tool rotational speed and traverse speed due to the fine grains, due to the dynamic recrystallisation, and an onion-ring structure, which improves the properties. Surface appearance and macrostructure results reveal that the weld produced at a higher tool rotational speed of 1800 rpm and moderate traverse speed of 100 mm/min leads to good surface appearance with a flawless weld. Furthermore, the welds produced at 1800 rpm/80mm/min and 1600rpm/120 mm/min of tool rotational and traverse combination show the highest values of microhardness in the probe region due to the exertion of higher stresses because of the round dome shape that deforms the grains to a higher extent, which increases the microhardness values.

Keywords- Process parameters, FSW, mechanical behavior, surface appearance, microhardness.

I. INTRODUCTION

Increasing demand for reducing weight in the automotive industry has prompted a significant interest in applications of lightweight materials, particularly aluminum alloys [1-2]. Friction Stir welding (FSW), invented by Thomas and his colleagues at The Welding Institute (TWI, Cambridge, United Kingdom) in 1991, is a rapidly maturing solid-state joining technique, involving frictional and adiabatic heating, plastic deformation (a combination of extrusion, forging, and shearing), and solid-state diffusion. Friction stir processing (FSP) was later developed by Mishra and his co-workers [3] based on the basic principles of FSW. FSP has been proven to be an effective and versatile metalworking technique for generating fine-grained microstructures and surface composites, e.g., for modifying the microstructures of Al-based alloys and Ni-Al bronze. [4-6]. For FSW, two parameters are very important: toolHowever, it should be noted that the frictional coupling of the tool surface with the workpiece is going to govern the heating. So, a monotonic increase in heating with increasing tool rotation rate is not expected, as the coefficient of friction at the interface will change with increasing tool rotation rate. In addition to the tool rotation rate and traverse speed, another important process parameter is the angle of the spindle or tool tilt with

respect to the workpiece surface [7-12]. A suitable tilt of the spindle towards the trailing direction ensures that the shoulder of the tool holds the stirred material by the threaded pin and moves material efficiently from the front to the back of the pin [13]. Further, the insertion depth of the pin into the workpieces (also called target depth) is important for producing sound welds with smooth tool shoulders. The insertion depth of the pin is associated with the pin height. When the insertion depth is too shallow, the shoulder of the tool does not contact the original workpiece surface. Thus, a rotating shoulder cannot move the stirred material efficiently from the front to the back of the pin, resulting in the generation of welds with an inner channel or surface groove [14-16]. Thus, it is difficult to produce a continuous defect-free weld. In these cases, preheating or an additional external heating source can help the material flow and increase the process window. On the other hand, materials with lower melting points, such as aluminum and magnesium, can be used to reduce [10, 17]. The weld properties are quite sensitive to the parameters at which welding is executed. Welding parameters affect the mechanical properties, energy consumption, quality, defect formation, and morphology of the weld [5, 18-20]. The parameters significantly influencing the microstructure and mechanical properties include rotational speed, traverse speed, and tool geometry [21]. Due to improper selection of parameters, numerous defects arise in the weldment, including kissing bonds, tunnelling, cracks, voids, flash, and lack of penetration [22]. This study addresses the optimization of welding parameters on FSW of AA1100 alloy using experimentation and Taguchi design of experiments. The Taguchi method is being employed, in which several factors can be optimized at the same time and quantitative data can be acquired with less experimental effort as compared to other methods [23-28]. Several attempts have been made to study the effects of different parameters on the microstructure and mechanical properties of Aluminum alloys. Pandey et al. [12] performed a study on defect formation during FSW on AA1100 alloy by varying traverse speed and rotational speed. The high rotational speed with lower traverse speed resulted in the formation of voids due to excessive heat generation, whereas craters and micro tunnels were found for low traverse and low rotational speed [28]. Mandal et al. [13] investigated the axial force during the plunging of a 12.5 mm thick AA2024 aluminum alloy. The peak load of 25 KN is recorded at the 5-second point, and diving is observed to be finished in 14 seconds. Kumar and Kailas [14] studied the impact of axial force on weld nugget defects. They get to the conclusion that the defect size reduces as the axial load increases. Han et al. [15] investigated the ideal conditions for friction stir welding 5083-O Al alloy. The 5083-O Al alloy's mechanical properties for friction stir welding (FSW) were assessed. The findings indicate that a weld flaw is seen at the start site in FSW at 800 r/min and 124 mm/min. Arora et al. [16] studied the design of a tool shoulder diameter using the maximization of supplied torque for traction as a basis. Using a numerical heat transfer and material flow model, the ideal tool shoulder diameter was calculated based on this approach. The shoulder sizes were adjusted to ϕ15, 18, and 21 mm, and the pin diameter was set at ϕ6 mm. The shoulder diameter of ϕ18 mm yielded the best weld joint strength. Bisadi et al. [17], In friction stir lap welding of 2.5 mm-thick AA 5083 to 3 mm-thick commercially pure copper sheets, claimed, in good agreement that extreme welding temperatures give rise to defective joints. Vahid et al. [18] studied the effect of probe shape and shoulder surface for EN AW-6061 alloy using six different tools. The results showed that the conical shoulder with a threaded square probe gave the highest tensile strength. Saeid et al. [19] made lap joints of AA1060 and copper sheets 4 and 3 mm thick, respectively, by a tool made of H13 with a shoulder diameter of 15 mm and a cylindrical threaded pin 15 mm in diameter and 6.5 mm in length. Galvao et al [20] worked on a heat-treatable (AA6082) and a non-heat treatable (AA5083) aluminium alloy. They were friction stir lap-welded to copper using the same welding parameters. Suresha et al. [21] utilized the Taguchi method and ANOVA analysis to perform the study for different probe profiles. Welding parameters, including RPM, heel plunge depth, and traverse speed, were used, and it was determined that RPM had a major effect on the tensile strength. K. Venkata Kalyani et al [22] This paper deals with the friction stir welding of AA6061-T6 Aluminium Alloy

by using H13 tool at different rotational speeds and welding feeds, and pin diameters. Experiments were conducted according to the L9 orthogonal array, which was suggested by Taguchi. Optimum parameters for optimum tensile strength, hardness, and ductility were found with the help of s/n ratios. Therefore, optimization of the input process parameter is required to achieve a good quality of welding. In this experiment, the effect of process parameters on the welded joint was studied, and the parameters were optimized by using the Taguchi method for tensile strength, hardness, and ductility. Assign the rank to each factor which are having more influence on the mean tensile strength, hardness, and ductility. Tamadon et al. [23] investigated the influence of the probe profile (of WC based tools), traverse speed, and rotational speed was investigated by Tensile strength and weld morphology were studied. Different structural defects were found, and results emphasised the need for parametric optimisation. Optimisation of traverse speed, Prasad et al. [24] executed the FSW parameters. Tilt angle, and rotational speed for percentage elongation and hardness for dissimilar friction stir welding between 5mm plates of EN AW-5083 and EN AW 6061 alloys. It was concluded that the major contributing parameter to percentage elongation and hardness at the stir zone was traverse speed. Dialmi et al. [25] studied defect formation in friction stir welding and found abnormal stirring and insufficient and excessive heat input to be the main causes of defect formation. Nakowong et al. [26] performed an optimization study on FSW butt-welded semi-solid EN AW-5083 alloy using the Taguchi method and ANOVA analysis for tensile strength and hardness. The considered parameters included traverse speed, rotational speed, and tool probe profile, and it was concluded that the traverse speed was the most influential parameter for tensile strength, whereas none of the parameters was significant for hardness. This work is carried out for joining heat-treated aluminum alloys in a butt joint configuration. In this study, the variable parameters that affect much are taken as input parameters as tool rotational speed and traverse speed by keeping tool tilt angle and tool geometry are kept constant. The output parameters are microhardness, tensile strength, and yield strength. All the experiments will be conducted on the Vertical Machining Centre (VMC). The Taguchi method based on L9 orthogonal array design of experiment is used, and depending upon the design, a total of 9 experiments are to be performed; The output parameters are measured with an accurate method. Hardness is measured in the Vickers hardness tester, and tensile stress and yield stress are measured using a universal bending machine.

II. MATERIALS AND METHODS

To set up the Friction Stir welding module, the foremost important thing is the fixture that can securely hold the welding plates and stop the rotary and translation motions is necessary for carrying out real experiments as shown in Fig.1.

Fig 1. Fixture set up for FSW over the CNC milling machine bed with clamped FSW welds were made using a vertical milling machine of the Hass Doosan Puma 240 (Make: USA. Over this vertical milling machine, a Friction Stir Welding arrangement was mounted. Range of RPMs from 500 to 10000 rpm and traverse speeds from 500 to 5000 mm/min, allows for a variety of experiments with welding and rotational speeds. Thin sheets of AA1100 aluminum alloy were cut using a power hacksaw into the required dimensions of 110 mm x 110 mm x 2 mm, which were subsequently milled. To build FSW joints, a square butt joint configuration has been created. To determine the impact of various FSW parameters on the mechanical properties of FSW joints, single-pass welding has been utilized to produce the joints using friction stir welding tools. Before welding and testing, no preprocessing treatment was applied. The joints were fabricated using non-consumable EN31 hardened steel. The cylindrical tool shoulder with

dome dome-shaped pin has been employed in friction stir welding. Figure 2 displays the pictorial representation of the FSW tool, and Figure 2 shows the FSW tool with dimensions, CAD model, and actual employed during the process. The chemical composition of the AA1100 aluminum alloy workpiece, which is a non-heat treatable series of aluminum alloy, and the non-consumable EN31 hardened steel tool are displayed in Table 1. A light optical microscope (TRUEMET DFC-295) in conjunction with an image analysis program has been used to perform macrograph analysis, as shown in Figure 3

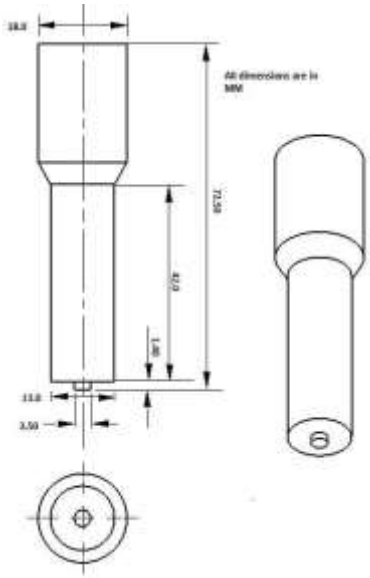

Composition	Weightage %
Silicon (Si)	0.760
Iron (Fe)	0.850
Magnesium (Mg)	0.0065
Manganese (Mn)	0.0059
Copper (Cu)	0.0096
Chromium (Cr)	0.0023
Remaining Aluminum	98.7

Table 2. FSW experimentation matrix

	Tool Rotational Speed, rpm		
Traverse Speed, mm/min	1400	1600	1800
80	1400/80	1600/80	1800/80
100	1400/100	1600/100	1600/100
120	1400/120	1600/120	1800/120

Fig 3 Light optical microscope (TRUEMET-DFC-295) with image analysis software.

The specimens for metallographic analysis have been prepared according to the standard metallographic procedure. The material behavior of the FSW-welded samples was assessed according to the different FSW welding parameter conditions. For this, the microhardness profiles of the FSW welds were measured in cross-sections of welded joints that were cut perpendicular to the weld line (welding direction). For measuring the Vickers microhardness, the Vickers microhardness testing equipment was employed. Vicker's microhardness was assessed using a 50 gmf (0.5 N) load and a 15-second dwell time. To ensure reliable findings, the sample should be cleaned and properly polished before the microhardness test. To study the tensile behavior of the FSW welds and base material, the tensile specimens were cut from the FSW welds using Wire Electrical Discharge Machining (WEDM) and then machined to the necessary proportions. The specimens for the Tensile Test and their 2D representation of the specimen with standard dimensions extracted from the FSW welded samples are shown in Figure 4. The tensile test specimens were prepared per the American Society for Testing of Materials (ASTM E8M-04).

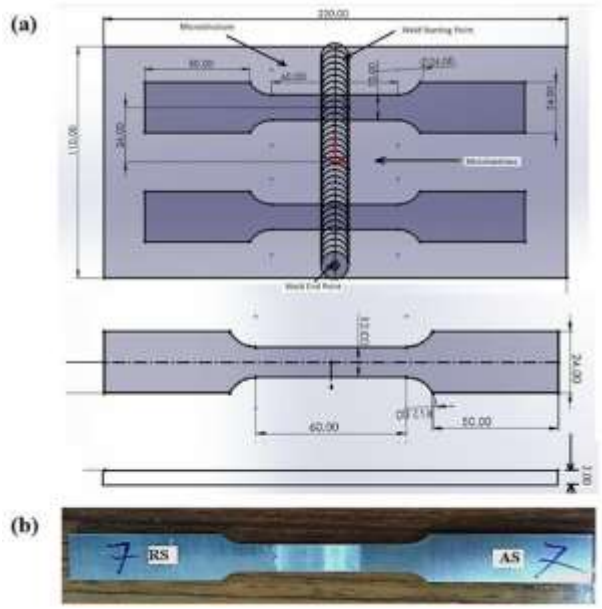

Fig 4. (a) Tensile test specimen with dimensions, (b) Actual Tensile test specimen

Tensile test was conducted in 100 kN, electro-mechanically controlled Universal Testing Machine (INSTRON). According to ASTM guidelines, the specimen is loaded at a strain rate of 2 mm/min, and an extensometer is fastened to it. This equipment is used for experiments with a ram rate of 2 mm/min. Ultimate tensile strength, maximum elongation, and area reduction are properties that can be directly determined with a tensile test.

III. RESULTS AND DISCUSSION

Tensile Behavior Evaluation

For tensile behavior evaluation, the stress-strain curve for the FSW weld produced at each welding parameter has been evaluated. From the result, it is inferred that the base matrix AA1100 aluminum alloy exhibits the ultimate tensile strength of 155 MPa with a yield strength of 75 MPa, and an elongation percentage of 12%. While the influence of FSW welding parameters on tensile behavior of each set of welds was evaluated followed for preparing the test specimens were prepared. The transverse tensile characteristics of FSW joints, including ultimate tensile strength, yield strength, percentage elongation, and joint efficiency, have been assessed as shown in Table 3. From Table 3, it has been seen that when the tool rotational speed was increased from 1400 rpm to 1800 rpm at constant traverse speed 80 mm/min, the FSW welds show significant improvement in UTS, YS and % elongation, which is due to proper consolidation of the deformed material and stir action induced by the FSW tool pin beneath the workpiece. Whi

Table 3. Mechanical properties of welded joints

Traverse speed, mm/min	Rotational Speed, rpm	UTS, MPa	Yield stress, MPa	% elongation	% Joint efficiency
80	1400	134.000	66.00	4.86	86.45
	1600	134.417	67.17	5.82	86.72
	1800	142.000	70.92	8.38	91.61
100	1400	137.663	68.67	6.30	88.81
	1600	136.750	66.25	6.38	88.22
	1800	**148.250**	**74.00**	**11.02**	**95.64**
120	1400	136.833	68.33	5.48	88.27
	1600	127.667	66.75	1.90	82.36
	1800	135.917	54.33	5.72	87.68

Therefore, it can be concluded that the tensile characteristics of the FSW joints were more influenced by the tool's rotational speed than the traverse speed [14,25]. The FSW welds produced at 1800 rpm and 100 mm/in of tool rotational speed and traverse speed outperformed the other joints in terms of tensile strength. When compared to traditional fusion welding, which has a low joint efficiency of no more than 50%, the joint efficiency is adequate even though the tensile strength values are lower than those of the base metal. Because of the domeshaped tool pin, it generates less heat, due to which the FSW welds have higher yield stress [31, 36]. Reduced temperature generation lowers the cooling rate, which causes joint brittleness; as a result, the graph's percentage of elongation falls [25, 37]. The second is that increased stirring in the nugget zone at high rotational speed and low traverse speed reduces particle size, increasing hardness and brittleness in the joint. For every set of rotational speed and traverse speed, the welds have higher ultimate tensile stress (127 MPa – 148 MPa) and percentage elongation (1.9 - 11) with joint efficiency (8295%) compared to the base material

(155 MPa, 75MPa and 12% of ultimate tensile strength, yield strength and % elongation, respectively). This is because the tool generates more heat, which results in a longer cooling period, which promotes grain growth and increases the material's ductility [21, 58-59]. The traverse speed (feed rate) of 100 mm/min is superior to the other two traverse speeds (80 mm/min and 120 mm/min) for the welds produced at 1800 rpm (148 MPa), than those produced at 1400 rpm (137 MPa) and 1600 rpm (136 MPa). With all traverse speeds (80, 100, and 120 mm/min), a rotational speed of 1800 rpm provides better ultimate and yield strength (74 MPa). The traverse speed of 120 mm/min provides minimum yield (66 MPa) and ultimate tensile strength (127MPa), especially for welds produced at rotational speeds of 1600 and 1800 rpm, respectively.

Macrostructure Analysis

The effects of FSW process parameters on the friction stirwelded joints' macrostructure reveal that weld quality and joint quality deteriorate when aluminum alloys are fused with flaws such as porosity, slag inclusion, solidification fractures, etc [38, 39]. The kissing bond, which is mostly caused by inadequate diving of the welding tool during FSW, typically indicates a partial residual of the unwelded butt surface beneath the stir zone. The kissing bond's mechanism is linked to the oxide layer's inadequate breakup caused by the contacting surfaces' inadequate stretch around the welding pin. It was found that the oxide layers on the original butt surfaces may be directly linked without the metallic bond between oxide-free surfaces in the root section of the weld because of the continuous oxide film that was created by inadequate stirring [25,40]. 3.3 Surface Appearance of Welded Plates

In the case of higher Tool rotational speed and lower traverse speed, as well as the combination of lower rotational speed and higher traverse speed resulted in poor weld surface morphology that causes a semicircular trail over the welded surface, the surface appearance of the welded samples is quite good or smooth. Downforce, or downward force in the Z-direction, is an additional element that influences the appearance of the weld surface [41-42]. Flash formation is moderate. When the tool rotates and moves along the joint line during welding, it pulls metal in the retreating side, where it accumulates and becomes a flash. The surface appearance of welded joints is shown in Figure 5. The samples' numbers with the respective parameters are mentioned below, Figure 5. The weld comprises a 13 mm area (same as the shoulder diameter), whereas the length of the welded plates is 110 mm. The intensity difference shows the non-homogeneity of the material. The dark lines show the lack of material, whereas the bright li

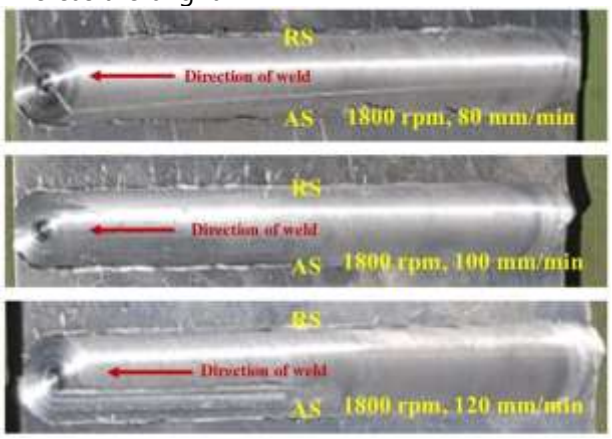

Fig 5. Surface appearance of FSW-welded samples

The heat generation increases with the increase in rotational speed and decreases with increasing traverse speed [28]. A certain combination of these parameters generates excess heat, due to which the material expands, and a certain amount of material is lost due to flashing (1400 rpm, 80 mm/min). When the tool moves forward, the material starts to cool down. The material cooling occurs in two possible ways: one from the surface to the atmosphere and the other by conduction in the material [25, 43].

3.4 Microhardness Evaluation

For all set of FSW welds produced at different tool rotational speed and traverse speed combinations reveals higher microhardness in the nugget zone, as shown in Figure 6. It has been observed that the FSW weld produces at 1800 rpm and 100 mm/min of tool rotational speed and traverse speed resulted in higher microhardness value 55 HV than FSW weld produced at other process parameters because it stirs more at a higher rotational speed, which produces fine grains, and it generates less temperature, or rapid cooling, which also produces fine grains, which is what causes high hardness and a decrease in the percentage of elongation [14,36, 44]. Figure 6 shows the Vickers microhardness profile

for FSW samples. The dashed lines show the probe region and the shoulder region. The zero position is the centreline of the welded plates. A "W" shaped trend is observed in the variation of microhardness, i.e., the value decreases in the welding region (shoulder area) with a small increase in the probe region

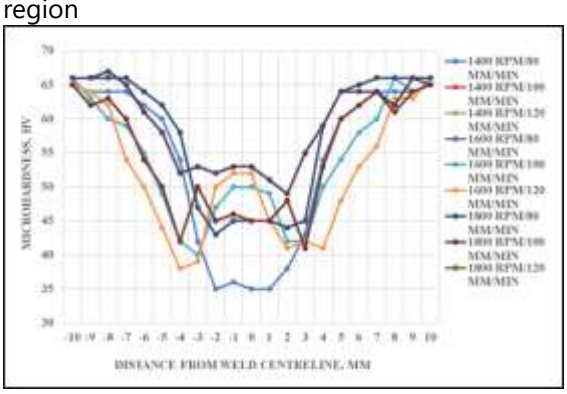

Fig 6. Vickers microhardness distribution of FSW welds produced at different process parameters.

As shown in Figure 6, samples 1800 rpm/80mm/min and 1600rpm/120 mm/min show the highest values in the probe region. This is due to at higher tool rotational speed and traverse speed, the probe exerts higher stresses due to the round dome shape and d

eforms the grains to a higher extent, which increases the hardness values [25, 45].

IV. CONCLUSIONS

The following conclusions have been drawn from this

investigation: -

1. Increase in tool rotational speed from 1400 rpm to 1800 rpm at constant traverse speed 80 mm/min show significant improvement in tensile properties of FSW welds due to proper consolidation of the deformed material and stir action, While, further increase in traverse speed to 100 mm/min leads to remarkable improvement with maximum 148 MPa UTS, 74 MPa yield strength, and 11.02% elongation with highest joint efficiency of 95.64% of FSW weld. The joint efficiency of most of the samples is around 70–80 % with the highest joint efficiency of 95.64% of FSW welds produced at 1800 rpm and 100 mm/min of tool rotational speed and traverse speed due to the fine grains, due to the dynamic recrystallisation, and an onion-ring structure, which improves the properties.
2. Surface appearance and macrostructure results reveal that the weld produced at a higher tool rotational speed, 1800 rpm, and moderate traverse speed, 100 mm/min, leads to good surface appearance with a flawless weld. While the heat generation increases with the increase in rotational speed and decreases with increasing traverse speed due to which material expands, and a certain amount of material is lost due to flashing (1400 rpm, 80 mm/min). As a result, the material contract due to the material loss in flashing and a certain linear defect (1800 rpm, 120 mm/min) occurs.
3. Microhardness results reveal that the welds produced at 1800 rpm/80mm/min and 1600rpm/120 mm/min of tool rotational and traverse combination show the highest values in the probe region. This is due to higher tool rotational speed and traverse speed; the probe exerts higher stresses due to the round dome shape and deforms the grains to a higher extent, which increases the microhardness values.

References

1. London B, Mahoney M, Bingel M, Calabrese M, Bossi R H, and Waldron D. 2003 Material flow in friction stir welding monitored with Al–SiC and Al–W composite markers. Friction stir welding and processing II (Warrendale, PA: TMS) pp 3–1
2. Huang G, Wu J, and Shen Y. 2018. A strategy for improving the mechanical properties of FSWed joints of non-heat-treatable Al alloys through a combination of water cooling and particle addition. J. Manuf. Process. 34 667–7
3. Fallahi A A, Shokuhfar A, Moghaddam A O, and Abdolahzadeh A 2017 Analysis of SiC nano-powder effects on friction stir welding of dissimilar Al-Mg alloy to A316L stainless steel, J. Manuf. Process. 30 418–3
4. K. Elangovana, V. Balasubramanian, "Influences of tool pin profile and traverse speed on the formation of friction stir processing zone in AA2219 aluminum alloy", Processing Technology, Volume 20, 2008, Pages 163–175.

5. H. Fujii, L. Cui, M. Maeda, K.Nogi, "Effect of tool shape on mechanical properties and microstructure of friction stir welded aluminum alloys" Materials Science and Engineering, Volume 419, Issues 1-2, 15 March 2006, Pages 25-31
6. A. Scialpi , L.A.C. De Filippis, P. Cavaliere "Influence of shoulder geometry on microstructure and mechanical properties of friction stir welded 6082 aluminum alloy" Material & Design, Volume 28, 2007, Pages1124– 1129.
7. I. Galvao, R.M. Leal, D.M. Rodrigues, A. Loureiro "Influence of tool shoulder geometry on properties of friction stir welds in thin copper sheets" Materials Processing Technology, Volume 213, 2013, Pages 129– 135.
8. Liguo Zhang, Shude Ji, Guohong Luan, Chunlin Dong, and Li Fu, "Friction Stir Welding of Al Alloy Thin Plate by Rotational Tool without Pin,"2011.
9. R.M. Leal, C. Leitao, A. Loureiro, D.M. Rodrigues, P. Vilac, "Material flow in heterogeneous friction stir welding of thin aluminum sheets: Effect of shoulder geometry" Science and Engineering, volume A 498, 2008, Pages 384–391.
10. H.R. Shercliff, P.A. Colegrove, Friction stir welding and processing, in: R. S. Mishra, et al., (Eds.), ASM International, Materials Park, OH,2007, pp. 187–217.
11. P. Cavalierea, A. Squillaceb, F. Panellaa, "Effect of welding parameters on mechanical and microstructural properties of AA6082 joints produced by friction stir welding" Materials Processing Technology, Volume 200, 2008, Pages 364–372
12. A. K. Pandey, V. Narayanan. Investigation of defect formation during friction stir welding of aluminum alloys. AIP Conference Proceedings 2273(1):050030, 2020
13. S. Mandal, J. Rice, A.Elmustafa, "Experimental and numerical investigation of the plunge stage in friction stir welding" Materials Processing Technology, Volume 203, Issues 1-3, 18 July 2008, Pages 411-419.
14. K. Kumar, S. Kailas, "On the role of axial load and the effect of interface position on the tensile strength of a friction stir welded aluminum alloy" Materials & Design, Volume 29, Issue 4, 2008, Pages 791-797.
15. M. Han, S. Lee, J. Park, S. Ko, Y. Woo, S. Kim "Optimum condition by mechanical characteristic evaluation in friction stir welding for 5083-O Al alloy" Nonferrous material Society, China, Volume 19, 2009, Pages 17-22.
16. A. Arora, A. De, and T. DebRoy, "Toward optimum friction stir welding tool shoulder diameter" Scripta materialia, Volume 64, 2011, pages 9-12.
17. H. Bisadi, A. Tavakoli, M. Tour Sangsaraki, K. Tour Sangsaraki, "The influences of rotational and welding speeds on microstructures and mechanical properties of friction stir welded Al5083 and commercially pure copper sheets lap joints" Materials and Design 43 (2013) pp.80–88
18. V. Moosabeiki, G. Azimi, M. Ghayoor. Influences of tool pin profile and tool shoulder curvature on the formation of the friction stir welding zone in AA6061 aluminium alloy. In Materials and Manufacturing Technologies XIV, vol. 445 of Advanced Materials Research, pp. 789–794. Trans Tech Publications Ltd, 2012.
19. I. Galvãoa, D. Verderab, D. Gestob, A. Loureiroa, D.M. Rodrigues"Influence of aluminium alloy type on dissimilar friction stir lap welding of aluminum to copper" Journal of Materials Processing Technology 213 (2013) pp 1920–1928
20. I. Galvãoa, R.M. Leala,b, D.M. Rodriguesa, A. Loureiro"Influence of tool shoulder geometry on properties of friction stir welds in thin copper sheets" Journal of Materials Processing Technology 213 (2013) pp 129–135
21. C.Devanathana,A.SureshBabu."Friction Stir Welding of Metal Matrix Composite using Coated tool" Procedia Materials Science 6 (2014) pp 1470 – 1475
22. K. Venkanta Kalyani, K.Sunil Ratna Kumar,K.V.P.P.Chandu, S. V. Gopala. "Optimizing the process parameters of friction stir butt welded joint on aluminium alloy AA6061-T6" International Journal of Research in Engineering and Technology. (Volume-03, issue-11)
23. A. Tamadon, A. Baghestani, M. E. Bajgholi. Influence of WC-based pin tool profile on

microstructure and mechanical properties of AA1100 FSW welds.
Technologies 8(2):34, 2020.
24. M. Prasad, K. Kumar Namala. Process parameters optimization in friction stir welding by ANOVA. Materials Today: Proceedings 5(2, Part 1):4824–4831, 2018. 7th International Conference of Materials Processing and Characterization, March 17-19, 2017.
25. N. Dialami, M. Cervera, M. Chiumenti. Defect formation and material flow in friction stir welding. European Journal of Mechanics - A/Solids 80:103912, 2020.
26. K. Nakowong, K. Sillapasa. Optimized parameter for butt joint in friction stir welding of semi-solid aluminum alloy 5083 using Taguchi technique. Journal of Manufacturing and Materials Processing 5(3):88, 2021.
27. K. Elangovan, V. Balasubramanian. Influences of tool pin profile and tool shoulder diameter on the formation of friction stir processing zone in AA6061 aluminium alloy. Materials & Design 29(2):362–373, 2008.
28. Avinash P, Manikandan, Arivazhagan, Devendranath Ramkumar, Narayanan," Friction stir welded butt joints of AA2014 T3 and AA7075 T6 Aluminium alloys"7th International Conference on Materials for advanced technology" Procedia Engineering 75(2014) pp 98-102
29. Bodaghi M and Dehghani K 2017 Friction stir welding of AA5052: the effects of SiC nano-particles addition Int. J. Adv. Manuf. Technol. 88 2651–60
30. C. Leitão, R. Louro, D.M. "Rodrigues Analysis of high temperature plastic behaviour and its relation with weldability in friction stir welding for aluminium alloys AA5083-H111 and AA6082-T6" Materials and Design 37 (2012) pp.402–409
31. V. John, R. Pant, S. Aggrawal, P. Agarwal. Parametric analysis and effect of tool on FSW joint of 6082 Al alloy by Taguchi method. International Journal of Mechanical and Production Engineering Research and Development 8(1):105–110, 2018
32. Y. Hwang, Z. Kang, Y. Chiou, H. Hsu, "Experimental study on temperature distributions within the workpiece during friction stir welding of aluminum alloys" Machine Tools and Manufacture, Volume 48, Issues 7-8, June 2008, Pages 778-787.
33. H. Fujii, L. Cui, M. Maeda, K.Nogi, "Effect of tool shape on mechanical properties and microstructure of friction stir welded aluminum alloys, Materials Science and Engineering, Volume 419, Issues 1-2, 15 March 2006, Pages 25-31
34. Singh T, Tiwari SK, Shukla DK (2020) Mechanical and microstructural characterization of friction stir welded AA6061-T6 joints reinforced with nano-sized particles. Materials Characterization. 159, 110047
35. Humphreys F (2001) Review grain and subgrain characterization by electron backscatter diffraction. J. mater. Sci. 36(16), 3833-3854.
36. Kumar K S A, Murigendrappa S M, Kumar H, and Shekhar H 2018. Effect of tool rotation speed on microstructure and tensile properties of FSW joints of 2024-T351 and 7075-T651 reinforced with SiC nanoparticle: The role of FSW single pass A.I.P. Conf. Proc 1943
37. Singh T, Tiwari SK, Shukla DK (2019) Friction-stir welding of AA6061-T6: The effects of Al2O3 nanoparticles addition. Results in Materials. 1, 100005
38. Mir MA, Islam SSU, Khan NZ, Ahmad B, Siddiquee AN (2024). Effect of processing parameters on microstructure and tensile strength of stainless steel, Reference Module in Materials Science and Materials Engineering,2024,
39. Singh T, Tiwari SK, Shukla DK (2019). Effect of nanosized particles on grain structure and mechanical behavior of friction stir-welded Al-nanocomposites. Proc Inst Mech Eng Part L. J Mater Des Appl. 234(2), 274-290.
40. Singh T, Tiwari SK, Shukla DK (2019). Processing parameters optimization to produce a nanocomposite using friction stir welding. Eng. Res. Express. 1, 025048.
41. Naghibi HY, Omidvar H, Nikoo MF (2018). Investigating the effects of traveling speeds and postweld heat treatment on the mechanical properties of nano-Al2O3-fortified AA6061-T6 friction stir welds. Proc. Inst. Mech. Eng. Part L: J. Mater. Des. Appl. 232(10), 816–28.

42. Mingzhi W, Hongchen L, Sainan G, Yun W, Ziqi W, Jian W, Li X, Yalin L, Jiangtao W (2024) Effects of rotational speed on microstructure, exothermic reactions, and mechanical properties of Al/Ni energetic structural materials prepared by hot pressing and friction stir processing, Journal of Materials Research and Technology, 29,2597-2607.
43. Sun YF, Fujii H (2011). The effect of SiC particles on the microstructure and mechanical properties of friction stir-welded pure copper joints. Mater. Sci. Eng. A. 528(16–17), 5470–5.
44. Singh T 2021 Processing of friction stir welded AA6061-T6 joints reinforced with nanoparticle, Results in Materials. 12 100210
45. Singh T, Tiwari S K, and Shukla D K 2020 Mechanical and microstructural characterization of friction stir welded AA6061-T6 joints reinforced with nano-sized particles Mater. Charact. 159 110047

Author's details

1. Raj Kumar Pathak, Research Scholar, Department of Mechanical Engineering, St. Soldier Institute of Engineering and Technology, Jalandhar, Punjab, India. rajnitesh528@gmail.com
2. Dr. Tanvir Singh, Assistant Professor, Department of Mechanical Engineering, St. Soldier Institute of Engineering and Technology, Jalandhar, Punjab, India. tanvirsingh3@gmail.com